

# Effects of flow shear on the ion temperature gradient modes in a high $\beta$ plasma slab

Zhe Gao<sup>a)</sup>

*Department of Engineering Physics, Tsinghua University, Beijing 100084, People's Republic of China*

J. Q. Dong

*Southwestern Institute of Physics, Chengdu 610041, People's Republic of China*

G. J. Liu and C. T. Ying

*Department of Engineering Physics, Tsinghua University, Beijing 100084, People's Republic of China*

(Received 26 August 2002; accepted 2 December 2002)

The integral eigenmode equations derived previously for the study of drift instabilities in a sheared slab plasma with arbitrary  $\beta$  (plasma pressure/magnetic pressure) are extended. These equations are used to investigate the effects of flow shear on the ion temperature gradient driven (ITG) modes. It is found that the destabilizing effect of a parallel velocity shear,  $V'_0$ , is weakened by the finite  $\beta$  effect, especially in case of weak magnetic shear. However, the perpendicular velocity shear,  $V'_E$ , still effectively stabilizes these modes even in high  $\beta$  regions. A large enough  $V'_E$  can completely stabilize the ITG mode at arbitrary  $\beta$ . In addition, the effect of  $V'_E$  is highly enhanced in weak magnetic shear regions. When the parallel flow coexists with the perpendicular flow, the comprehensive flow effect depends on the relative sign of these velocity shears. The modes with higher growth rates may be stabilized by a smaller  $V'_E$  for  $V'_0 V'_E > 0$ . © 2003 American Institute of Physics. [DOI: 10.1063/1.1541023]

## I. INTRODUCTION

Strong sheared flows are observed accompanying the formation of transport barriers in improved confinement experiments<sup>1–3</sup> in tokamaks. The influence of sheared flow on plasma microinstabilities has been one of the most interesting topics in recent decades. The  $\mathbf{E} \times \mathbf{B}$  velocity shear is believed<sup>4</sup> to play a central role in improved confinement experiments. There are two themes associated with velocity shear effects on the reduction of anomalous transport, i.e., the nonlinear decorrelation of turbulence and the linear stabilization of microinstabilities.

Since the ion temperature gradient driven (ITG) mode has been considered<sup>5–7</sup> as a candidate responsible for the anomalous ion transport in tokamak plasmas, numerous theoretical studies<sup>8–14</sup> on the ITG mode have been performed in the presence of sheared flows. The parallel<sup>8,9</sup> and perpendicular<sup>10,11</sup> sheared flows were considered separately and simultaneously<sup>12–14</sup> in a slab configuration. Separately, the parallel velocity shear tends to destabilize while the perpendicular velocity shear with a sufficiently large value stabilizes the modes. In addition, the study<sup>12</sup> including both types of flows shows that the combined effect of the flows can be stabilizing or destabilizing, depending on the relative sign of the parallel and perpendicular velocity shears. Nevertheless, the ITG modes are completely stabilized for sufficiently large values of the perpendicular velocity shear regardless of the signs.

Most previous studies<sup>8–14</sup> are focused on the electrostatic modes. However, finite  $\beta$  values were obtained in im-

proved confinement experiments.<sup>15</sup> Moreover, in advanced confinement devices, such as a spherical torus,  $\beta$  can reach much higher values.<sup>16,17</sup> In high  $\beta$  plasmas, the coupling of the slab ITG modes to the Alfvén waves, the magnetic gradient drift, and the electron dynamics have to be taken into account. In an early study<sup>18</sup> of the Kelvin–Helmholtz instabilities in high  $\beta$  plasmas, however, the two-fluid model was employed, and the effects of the temperature gradients and the perpendicular flow were not considered.

Using the kinetic theory, Gao *et al.*<sup>19</sup> investigated the effects of the parallel velocity shear and the parallel current on the local ITG mode in high  $\beta$  plasmas. It turns out that a finite  $\beta$  can not only weaken the driving mechanism of the parallel velocity shear but also reverses the current effect from weakly destabilizing to stabilizing. However, since the parallel wave number is fixed in the local theory, the eigenvalue depends on the signs of the flow parameters. Moreover, the effects of the magnetic shear and perpendicular sheared flow cannot be analyzed in the local model.

Recently, Gao *et al.*<sup>20</sup> developed a set of integral equations to study drift instabilities in arbitrary  $\beta$  plasmas with sheared slab magnetic configuration. Both components of the perturbed vector potential,  $\tilde{A}_\parallel$  and  $\tilde{A}_\perp$ , are considered together with the perturbed scalar potential  $\tilde{\phi}$  in the model, as well as the magnetic gradient drift effects. This model is extended to include the sheared flows in the present work. The effects of the parallel and perpendicular sheared flows are investigated using the extended model.

The organization of this paper is as follows. The extended integral eigenmode equations are presented in Sec. II. Simple analysis of sheared flows in the equations is per-

<sup>a)</sup>Electronic mail: gaozhe97@mails.tsinghua.edu.cn

formed in Sec. III. Numerical results are described in Sec. IV. Section V is devoted to summary and discussion.

## II. INTEGRAL EIGENMODE EQUATIONS IN THE PRESENCE OF SHEARED FLOWS

We consider a sheared magnetic field with a gradient  $\mathbf{B}(x) = B_0[\hat{z}(1 + x/L_B) + \hat{y}(x/L_s)]$ , where  $L_s$  and  $L_B$  are the scale lengths of the magnetic shear and the magnetic gradient, respectively. The magnetic gradient is related to the pressure profile by the static equilibrium condition:  $L_n/L_B = \sum_{j=i,e}(\beta_j/2)(1 + \eta_j)$ . Here,  $L_n^{-1} = -(1/n_j)dn_j/dx$ ,  $\eta_j = d \ln T_j/d \ln n_j$ , and  $\beta_j = 8\pi n_j T_j/B^2$ .

The equilibrium distribution functions for the electrons and the ions in the presence of the radial electrical field  $E(x)\mathbf{x}$ , magnetic field  $\mathbf{B}(x)$ , and parallel flow  $V_0(x)$  can be written as<sup>11</sup>

$$f_0 = g(X_g) \frac{n(X_g)}{\pi^{3/2} v_t^3} \exp\left[-\frac{v_x^2 + (v_y - V_E)^2 + (v_z - V_0)^2}{v_t^2}\right]. \quad (1)$$

Here,  $v_t = \sqrt{2T(X_g)/m}$ ,  $V_E = -cE(X_g)/B$ ,  $V_0 = V_0(X_g)$ ,  $X_g = x - v_y/\Omega$  is the radial coordinate of guiding center and  $\Omega = -qB/mc$  is the gyro-frequency. The normalization condition,  $\int f_0 d\mathbf{v} = n(x)$ , indicates that  $g(X_g)$  is the reciprocal of the Jacobian determinant of the transformation from the lab coordinates to the guiding center coordinates. So the  $g(X_g)$  can be eliminated by the coordinates transformation.

We introduce three fluctuating scalar fields:  $\tilde{\phi}$ ,  $\tilde{A}_1(=\tilde{\mathbf{A}}\cdot\mathbf{b})$ , and  $\tilde{A}_2(=(\tilde{\mathbf{A}}\times\hat{\mathbf{e}}_\perp)\cdot\mathbf{b})$ , where all perturbed quantities have the form  $\tilde{p}(\mathbf{r},t) = p(x)\exp(ik_y y - i\omega t)$ ,  $p(x) = 1/\sqrt{2\pi} \int p(k)\exp(ikx)dk$ ,  $\hat{\mathbf{e}}_\perp = \mathbf{k}_\perp/|k_\perp|$ ,  $\mathbf{k}_\perp = k_y\hat{y} + k_x\hat{x}$ , and  $\mathbf{b} = \mathbf{B}/B$ . For fluctuations with  $\omega \ll |\Omega_j|$  and  $k_\perp \lambda_d \ll 1$ , the linear eigenmode equations include the quasineutrality condition

$$\begin{aligned} \sum_j \frac{q_j^2 n_j}{T_j} \left\{ \hat{\phi}(k) + \frac{V_{0j}}{v_{te}} \hat{A}_1(k) + \left(\frac{1}{2\pi}\right) \int dk' \int dx \right. \\ \times \exp[i(k' - k)x] \left[ L_j(0,0,0,0) \left( \hat{\phi}(k') + \frac{V_{0j}}{v_{te}} \hat{A}_1(k') \right) \right. \\ \left. \left. + \frac{v_{tj}}{v_{te}} L_j\left(0,1,\frac{1}{2},0\right) \hat{A}_2(k') + \frac{v_{tj}}{v_{te}} L_j(0,0,0,1) \hat{A}_1(k') \right] \right\} = 0, \quad (2) \end{aligned}$$

the parallel components of the Ampère's law

$$\begin{aligned} \hat{A}_1(k) - \sum_j \frac{\beta_j}{2\pi b_j} \left\{ 2\pi \frac{V_{0j}}{v_{tj}} \left( \hat{\phi}(k) + \frac{V_{0j}}{v_{te}} \hat{A}_1(k) \right) \right. \\ \left. + \int dk' \int dx \exp[i(k' - k)x] \right. \\ \left. \times \left[ \frac{v_{te}}{v_{tj}} \left( L_j(0,0,0,1) + \frac{V_{0j}}{v_{tj}} L_j(0,0,0,0) \right) \hat{\phi}(k') \right. \right. \\ \left. \left. + \left( L_j\left(0,1,\frac{1}{2},1\right) + \frac{V_{0j}}{v_{tj}} L_j(0,0,0,0) \right) \hat{A}_2(k') \right] \right\} = 0, \end{aligned}$$

$$\begin{aligned} + \left( L_j(0,0,0,2) + 2 \frac{V_{0j}}{v_{tj}} L_j(0,0,0,1) \right. \\ \left. + \frac{V_{0j}^2}{v_{tj}^2} L_j(0,0,0,0) \right) \hat{A}_1(k') \Bigg\} = 0, \quad (3) \end{aligned}$$

and the perpendicular components of the Ampère's law

$$\begin{aligned} \hat{A}_2(k) - \sum_j \frac{\beta_j}{2\pi b_j} \left\{ \int dk' \int dx \exp[i(k' - k)x] \right. \\ \times \left[ \frac{v_{te}}{v_{tj}} L_j\left(1,0,\frac{1}{2},0\right) \hat{\phi}(k') + L_j(1,1,1,0) \hat{A}_2(k') \right. \\ \left. \left. + L_j\left(1,0,\frac{1}{2},1\right) \hat{A}_1(k') \right] \right\} = 0. \quad (4) \end{aligned}$$

Here,

$$\begin{aligned} L_j(m,n,s,l) = \left(\frac{-q_j}{|q_j|}\right)^{m+n} \int_0^{+\infty} dt t^s \\ \times \exp(-t) J_m(\sqrt{2b_j t}) J_n(\sqrt{2b'_j t}) \\ \times \frac{\omega_{*j}}{\omega - \omega_{Djt}} K_{ij}, \quad (5) \end{aligned}$$

$$\begin{aligned} K_{0j} = \left(\frac{\omega_{0j}}{\omega_{*j}} - 1\right) [\xi_j Z(\xi_j)] - \eta \left[ \xi_j^2 + \left(\xi_j^2 - \frac{1}{2}\right) \xi_j Z(\xi_j) \right] \\ - \eta_j(t-1) [\xi_j Z(\xi_j)] + 2 \frac{L_n}{v_{tj}} \frac{\partial V_{0j}}{\partial x} \frac{k_\parallel}{|k_\parallel|} \\ \times \xi_j [1 + \xi_j Z(\xi_j)] \\ + 2 \frac{L_n}{v_{tj}} \frac{\partial V_E}{\partial x} \frac{ik'}{k'_\perp} \left[ t^{1/2} \frac{-q_j}{|q_j|} \frac{-J_n(\sqrt{2b'_j t})}{J_n(\sqrt{2b_j t})} \right. \\ \left. + \frac{\delta}{\sqrt{2b'_j}} \right] \xi_j Z(\xi_j), \quad (6) \end{aligned}$$

$$K_{1j} = \frac{k_\parallel}{|k_\parallel|} \xi_j \left[ K_{0j} + \left(\frac{\omega_0}{\omega_{*j}} - 1\right) - \eta(t-1) \right], \quad (7)$$

$$K_{2j} = \frac{k_\parallel}{|k_\parallel|} \xi_j K_{1j}, \quad (8)$$

$\omega_{*j} = (k_y T_j)/(\Omega_j m_j L_n)$ ,  $\omega_{Dj} = -\omega_{*j} L_n/L_B$ ,  $b_j = k_\perp^2 \rho_j^2/2$ ,  $b'_j = k_\perp'^2 \rho_j^2/2$ ,  $\rho_j = v_{tj}/\Omega_j$ ,  $\xi_j = (\omega - \omega_{Djt})/|k_\parallel| v_{tj}$ ,  $k_\parallel = (x/L_s)k_y$ ,  $k_\perp^2 = k_y^2 + k_x^2$ ,  $k_\perp'^2 = k_y^2 + k_x'^2$ ,  $\hat{\phi} = \phi$ ,  $\hat{A}_2 = i v_{te} A_2/c$ ,  $\hat{A}_1 = -v_{te} A_1/c$ , and  $Z(\xi)$  is the plasma dispersion function. In Eq. (6),  $\delta$  equals one and zero when used in  $K_{0j}$  in terms multiplied by  $\hat{A}_2$  and by the other terms, respectively.

This model governs the behavior of these modes driven by temperature gradients and sheared flows in arbitrary  $\beta$  plasmas. Both the perturbed magnetic field and the magnetic gradient effect are considered in the equations. Moreover, kinetic effects such as particle-wave interaction, transit effect, and finite Larmor radius effect are taken into account for both ions and electrons. The integral equation formula-

tion is quite general and valid for modes in the  $|\rho_i \partial/\partial x| \sim O(1)$  regime. As the sheared flow terms are eliminated, the model reduces to the eigenmode equations derived by Gao et al.<sup>20</sup> to analyze the high  $\beta$  ITG mode. Also, the assumption of the validity of local treatment ( $k=k'=0$ ,  $k_{\parallel}=\text{const}$ ) simplifies Eqs. (2)–(4) to the local dispersion equations in Gao et al.<sup>19</sup>

### III. SIMPLE ANALYSIS OF SHEARED FLOWS

Expanding the sheared flows and neglecting the higher order derivatives, we obtain  $V_{0j}(x) = V_{0j}(0) + V'_{0j}x$ ,  $V_E(x) = V_E(0) + V'_E x$ . In the following, the ion flow velocities  $V_{0i}(0) = V_E(0) = 0$  are used since the emphasis is placed on the effects of the flow shears. In this case the effects of a parallel flow and a toroidal flow should be equivalent. The electron parallel flow is assumed to fully carry the current, that is,  $j = -neV_{0e} \equiv neu$ . Then, four flow parameters are introduced:  $V'_0 \equiv V'_{0i}$ ,  $V'_E$ ,  $u$ , and  $u'$ . The corresponding dimensionless quantities are  $\hat{V}'_0 = L_n V'_0 / v_{ti}$ ,  $\hat{V}'_E = L_n V'_E / v_{ti}$ ,  $\hat{u} = u / v_{ti}$ , and  $\hat{u}' = L_n u' / v_{ti}$ .

In the eigenmode equations, the flow shears and current affect the mode in two different ways. One is through the explicit dependencies in Eqs. (2)–(4), the other is through the argument of the plasma dispersion function,  $\xi_j$ . Substituting the expansion of sheared flows and the expression  $k_{\parallel} = (x/L_s)k_y$  into the  $\xi_j$ , we get

$$\xi_j = \frac{L_s}{L_n} \frac{\rho_j}{|x|} \left( \frac{\omega - \omega_{Djt}}{2\omega_{*j}} - \frac{L_n V'_E}{v_{tj}} \frac{x}{\rho_j} + \frac{L_n}{L_s} \frac{u_j}{v_{tj}} \frac{x}{\rho_j} \right) - \frac{x}{L_n} \frac{L_n V'_{0j}}{v_{tj}}, \quad (9)$$

where  $u_j$  equals  $u$  and zero for electrons and ions, respectively.

Since the eigenmode structure of microinstabilities is usually several gyro-radius wide, that is,  $x \sim \rho_i$ , the last term in Eq. (9) is of the order of  $\rho_i/L_n$ . As a result, the parallel velocity shear does not contribute to the plasma dispersion function, but affects the stability of the modes through the explicit dependencies in Eqs. (2)–(4), more precisely, through the fourth term in Eq. (6). The effects of a parallel velocity shear on the local mode have been investigated in our earlier work, which shows that a finite  $\beta$  weakens the destabilizing effect of  $V'_0$ .<sup>19</sup>

The current appears only in the expression of  $\xi_j$ , Eq. (9), in electrostatic cases. Obviously, the current can change the value of  $\xi_j$  significantly only when  $u \sim v_{te}$ . It is why only a large current of the order of  $nev_{te}$  can excite the current-driven drift instabilities.<sup>21</sup> However, the effect of the current also appears explicitly for finite  $\beta$  plasmas. This explicit dependence arises from the current response to different mean transfer velocities of the density fluctuations for ions and electrons,  $\tilde{n}(V_{0i} - V_{0e})$ . Finite  $\beta$  enhances the explicit stabilizing effect, then reverses the effect of the current from destabilizing to stabilizing.<sup>19</sup>

The perpendicular velocity shear affects the mode mainly by changing the value of  $\xi_j$ . This effect is strengthened at weak magnetic shear since the change of  $\xi_j$  due to a

$V'_E$  is proportional to the  $L_s/L_n$ . Moreover, it is seen from Eq. (9) that the  $V'_E$  effect depends on the mode structure and the direction of mode frequency. The explicit dependence of  $V'_E$ , the last term in Eq. (6), is kept in the eigenmode equations. This dependence is similar to the explicit dependence of  $V'_0$ , but is smaller than the latter, especially in the case of  $k \ll k_{\perp}$  or  $k_{\perp} \rho_i < 1$ . Numerical results in Sec. IV indicate that the influence of this explicit dependence is very weak indeed. It may be the reason that most previous works<sup>12–14</sup> omitted the explicit dependence of  $V'_E$ .

In the local model,<sup>19</sup> the eigenvalue does not change when the signs of flow parameters and  $k_{\parallel}$  are simultaneously reversed, that is,  $\omega(k_{\parallel}, V'_0, u, u') = \omega(-k_{\parallel}, -V'_0, -u, -u')$ . This relation can be applied to the nonlocal model with minor changes:

$$\begin{aligned} \omega(V'_0, V'_E, u, u') &= \omega(-V'_0, -V'_E, -u, -u'), \\ Q(x, V'_0, V'_E u, u') &= Q(-x, -V'_0, -V'_E -u, -u'), \\ Q &= \phi, A_2, A_{\parallel}. \end{aligned} \quad (10)$$

These relations are also given in Artun and Tang<sup>12</sup> for electrostatic modes, and are still valid for electromagnetic modes.

### IV. NUMERICAL RESULTS

The integral equations, Eqs. (2)–(4), are solved using the Raleigh–Ritz technique. When the effect of one flow parameter is examined, the other flow parameters are null unless the coexistence of flows is mentioned. Besides the flow parameters, the other parameters are  $\eta_e = 2$ ,  $\eta_i = 2$ ,  $T_e/T_i = 1$ ,  $m_i/m_e = 1836$ , and  $L_n/L_s = 0.1$  unless otherwise stated. For convenience, all the lengths have been normalized to  $|\rho_i|$  in the following.

#### A. Parallel sheared flow effects

Shown in Fig. 1 are the mode frequencies and growth rates as functions of  $\hat{V}'_0$  for different  $\beta$  values. The parallel velocity shear is destabilizing but its effect is dramatically reduced at higher  $\beta$  ( $\beta_e \sim 5\%$ ). In other words, the finite  $\beta$  stabilizing effect is dramatically enhanced in plasmas with parallel velocity shear. Moreover, a weak magnetic shear enhances the potential of  $\beta$  to weaken the parallel velocity shear effect. Figure 2 gives the mode frequencies and growth rates as functions of  $L_n/L_s$  for different  $\beta$  values.  $\hat{V}'_0 = 0$  and 0.4 are used. For  $\beta = 0$ , the growth rates for  $\hat{V}'_0 = 0$  and 0.4 are significantly different while the differences are negligible for  $\beta_e = 0.005$  and 0.05 at weak magnetic shear ( $L_n/L_s \leq 0.05$ ).

The parallel velocity shear destroys the symmetry in mode structure. Figure 3 shows that the mode structure shifts toward the  $+x$  direction at a positive  $\hat{V}'_0$ .

Another two parallel flow parameters are the parallel current and current gradient. Numerical results from the nonlocal model confirm the previous results of the local model.<sup>19</sup> As  $\beta$  increases, the current effect changes from being weakly destabilizing to stabilizing and finally becomes negligible. Figure 4 shows that a large current can stabilize the ITG mode at a moderate  $\beta$  value. Local results<sup>19</sup> also indicate that

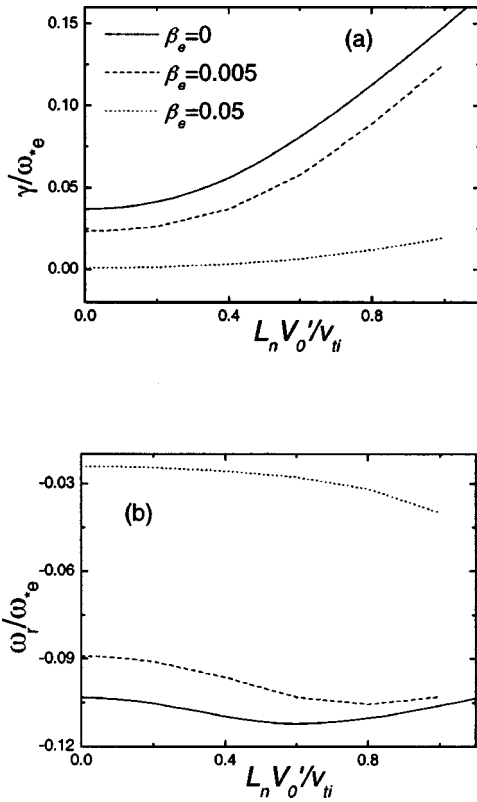


FIG. 1. Mode growth rate (a) and frequency (b) vs  $\hat{V}'_0$  for  $\eta_i = \eta_e = 2.0$ ,  $m_i/m_e = 1836$ ,  $T_e/T_i = 1$ ,  $L_n/L_s = 0.1$ ,  $k_y = 1$ , and  $\hat{V}'_E = \hat{u} = \hat{u}' = 0$ . The solid, dashed, and dotted lines denote the results for  $\beta_e = 0, 0.005$ , and  $0.05$ , respectively.

the current gradient effect is destabilizing at finite  $\beta$ , which is nearly opposite to the current effect. The line with crosses in Fig. 4 also reveals this trend. But here, the effects of the current and current gradient are very weak. In other words, the current that is needed to influence the stability properties of the mode is so large, above  $0.1 ne v_{te}$ , that it is beyond the currents in typical tokamaks. For example, in a plasma with  $n = 10^{20} \text{ m}^{-3}$ ,  $T_e = 10 \text{ keV}$ ,  $j = 1 \text{ MA m}^{-2}$ , the electron drift velocity which carries the current is  $6 \times 10^4 \text{ m s}^{-1}$ , while the electron thermal velocity is about  $4 \times 10^7 \text{ m s}^{-1}$ .

## B. Perpendicular sheared flow effects

The effect of perpendicular flow shear on the ITG mode is shown in Fig. 5. Unlike the effect of parallel flow shear, the effect of  $\hat{V}'_E$  is not weakened at finite, even high  $\beta$ . The initial rise in  $\hat{V}'_E$  causes a slow increase in the growth rate and a decrease in the frequency. After the frequency approximately reverses its direction, any further increase of  $\hat{V}'_E$  causes a sharp decrease in the growth rate. Then, the mode is fully stabilized by a finite  $\hat{V}'_E$  at arbitrary  $\beta$ . Figure 5 also shows the influence of the fourth term in Eq. (6) on the electrostatic mode. The destabilizing effect of this explicit  $\hat{V}'_E$  term is similar to but weaker than the effect of parallel velocity shear. At finite  $\beta$ , this destabilizing effect is weakened and can be omitted.

Magnetic shear strongly influences the  $\hat{V}'_E$  effect as is analyzed in Sec III. Figure 6 shows the mode frequencies

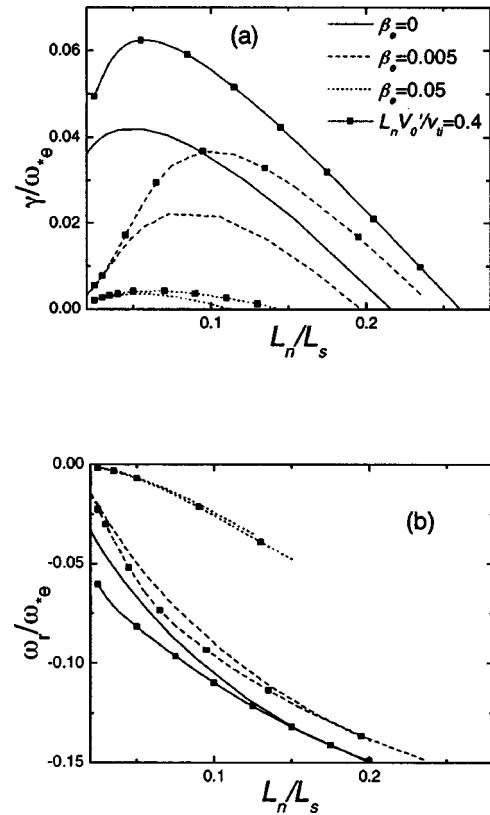


FIG. 2. Mode growth rate (a) and frequency (b) vs  $L_n/L_s$ . The lines without symbols denote the results for  $\hat{V}'_0 = 0$  and those with squares denote the results for  $\hat{V}'_0 = 0.4$ . The other parameters and denotations are the same as in Fig. 1.

and growth rates as functions of  $L_n/L_s$  for different  $\hat{V}'_E$  values at  $\beta_e = 0.005$  and  $0.05$ , respectively. In the weak shear region, a small  $\hat{V}'_E$  can stabilize the mode. However, in the strong shear region a larger  $\hat{V}'_E$  is required since the growth rate increases with  $\hat{V}'_E$  at the beginning. At moderate  $\beta$  ( $\beta_e = 0.005$ ), the  $\hat{V}'_E$  effect is reduced by a strong magnetic shear, which is similar to the electrostatic case ( $\beta_e = 0$ ).<sup>13</sup> However, at high  $\beta$  ( $\beta_e = 0.05$ ) and strong magnetic shear, it can be clearly seen that the mode is excited by a finite  $\hat{V}'_E$  and then stabilized by a larger  $\hat{V}'_E$ .

The effects of  $\hat{V}'_E$  on the modes of different poloidal wave vectors are shown in Fig. 7 at  $\beta_e = 0.005$  and  $0.05$ , respectively. In the long wavelength, small  $k_y$ , regime, the growth rate almost monotonously decreases with an increasing  $\hat{V}'_E$ , while in the large  $k_y$  regime the growth rate increases at the beginning and then decreases as  $\hat{V}'_E$  increases. In other words, the shorter wavelength mode can be excited by a finite  $\hat{V}'_E$  and then stabilized by a large enough  $\hat{V}'_E$ . This trend is more obvious at high  $\beta$ .

The increase of the  $\eta_i$  threshold due to finite  $\hat{V}'_E$  also embodies the stabilizing effect of  $\hat{V}'_E$ . For example, at  $\beta_e = 0.005$ , the  $\eta_i$  threshold values at  $\hat{V}'_E = 0, 0.08$ , and  $0.12$  are about  $0.97, 1.45$ , and  $1.75$ , respectively. However, the change of the  $\eta_i$  threshold due to finite  $\hat{V}'_0$  is not significant when  $\hat{V}'_0$  is less than  $0.4$ . This is in agreement with the previous electrostatic results.<sup>12,13</sup> The perpendicular velocity

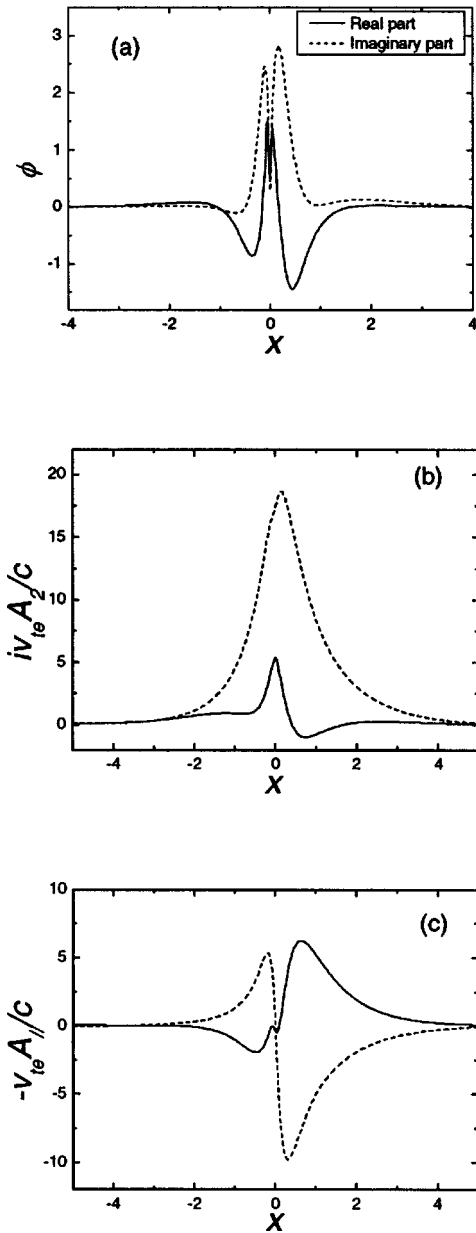


FIG. 3. Mode structure for  $\beta_e=0.05$  and  $\hat{V}'_0=0.4$ : (a)  $\phi(x)$  vs  $x$ ; (b)  $A_2(x)$  vs  $x$ ; (c)  $A_{||}(x)$  vs  $x$ . The other parameters are the same as in Fig. 1.

shear also destroys the symmetric mode structure. The mode structure shifts toward the  $+x$  direction at positive  $\hat{V}'_E$ .

**C. Coexistence of parallel and perpendicular flows**

Artun and Tang<sup>12</sup> studied the combined effects of parallel and perpendicular sheared flows on electrostatic modes. It is found that the flow effect is stabilizing or destabilizing depending on the relative sign of the parallel and perpendicular velocity shears and that the modes are completely stabilized for sufficiently large values of the perpendicular velocity shear regardless of the shear signs. This conclusion is also verified in our results for electrostatic modes. Moreover, it is also valid for electromagnetic modes in finite or high  $\beta$  plasmas, as shown in Figs. 8 and 9. As  $\hat{V}'_0\hat{V}'_E>0$ , the mode has a relatively high growth rate but is easily stabilized by a rela-

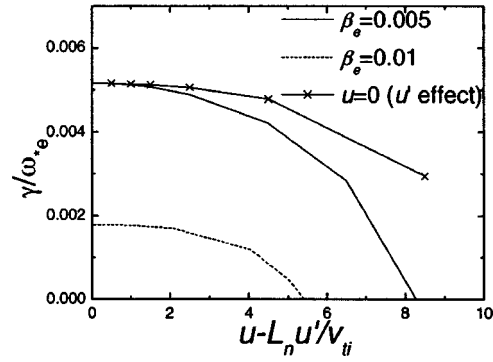


FIG. 4. Mode growth rate vs  $\hat{u}-\hat{u}'$ . The solid and dashed lines denote the results for  $\beta_e=0.005$  and  $0.01$ , respectively. The lines without symbols and with crosses denote the results for  $\hat{u}'=0$  and  $\hat{u}=0$ , respectively.  $\hat{V}'_0=0$  and the other parameters are the same as in Fig. 1.

tively small  $\hat{V}'_E$ . By contrast, the mode has a relatively low growth rate but is stabilized by a relatively large  $\hat{V}'_E$  for  $\hat{V}'_0\hat{V}'_E<0$ . It is because the  $\hat{V}'_E$  effect is enhanced by a  $\hat{V}'_0$  with the same sign. This enhancement causes the growth rate to reach a higher level when the growth rate increases with  $\hat{V}'_E$  in the small  $\hat{V}'_E$  regime. At the same time, it accelerates the stabilizing course when the growth rate begins to decrease with further increasing of  $\hat{V}'_E$ . The trend is also more obvious at higher  $\beta$ .

The mechanism could be illuminated through the mode structures for different signs of  $\hat{V}'_0\hat{V}'_E$ . Since  $\hat{V}'_E$  is multiplied

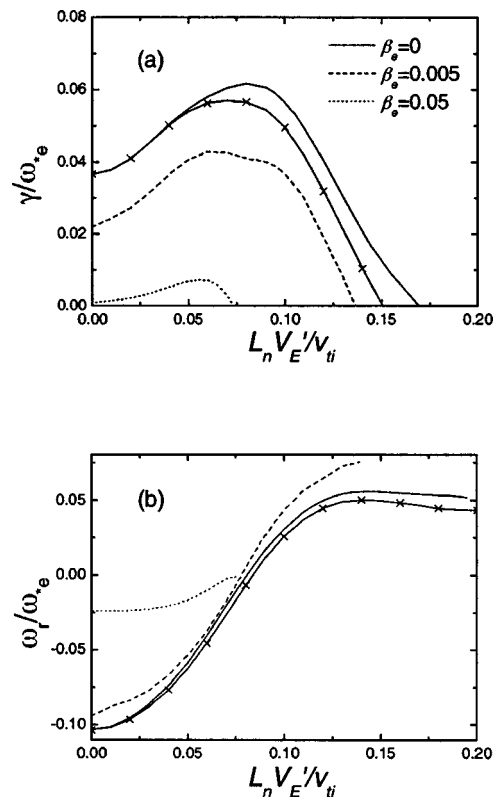


FIG. 5. Mode growth rate (a) and frequency (b) vs  $\hat{V}'_E$ . The line with crosses denotes the results from the model without the explicit  $\hat{V}'_E$  term.  $\hat{V}'_0=0$  and the other parameters and denotations are the same as in Fig. 1.

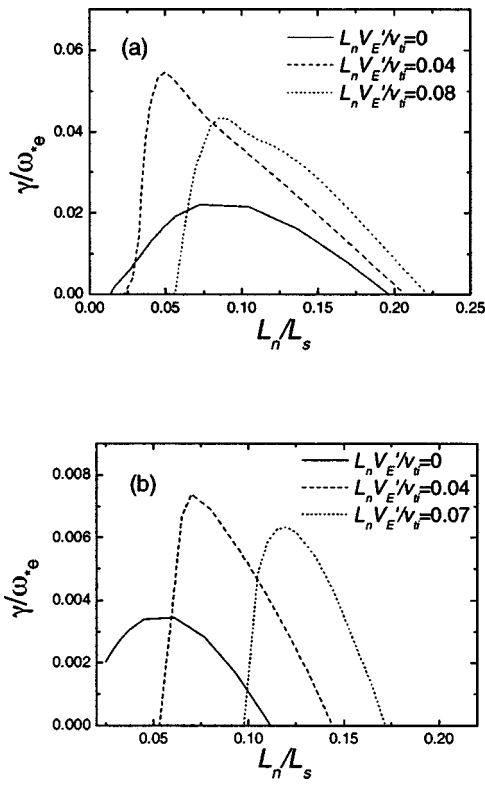


FIG. 6. Mode growth rate vs  $L_n/L_s$  for different  $\hat{V}'_E$  values and  $\beta_e = 0.005$  (a) and  $0.05$  (b), respectively.  $\hat{V}'_0 = 0$  and the other parameters are the same as in Fig. 1.

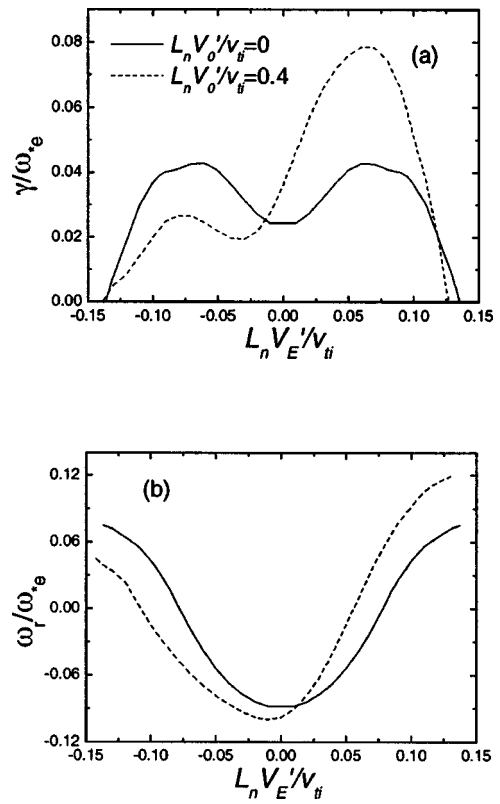


FIG. 8. Mode growth rate (a) and frequency (b) vs  $\hat{V}'_E$  for  $\beta_e = 0.005$ . The solid and dashed lines denote the results for  $\hat{V}'_0 = 0$  and  $0.4$ , respectively. The other parameters are the same as in Fig. 1.

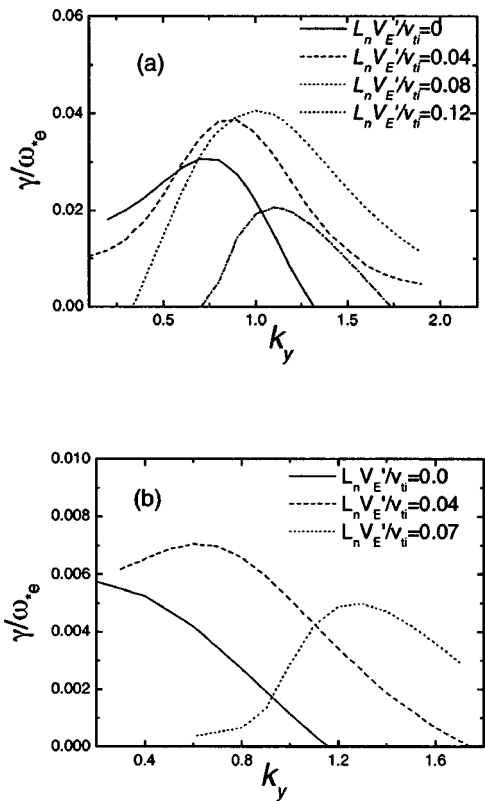


FIG. 7. Mode growth rate vs  $k_y$  for different  $\hat{V}'_E$  values and  $\beta_e = 0.005$  (a) and  $0.05$  (b), respectively.  $\hat{V}'_0 = 0$  and the other parameters are the same as in Fig. 1.

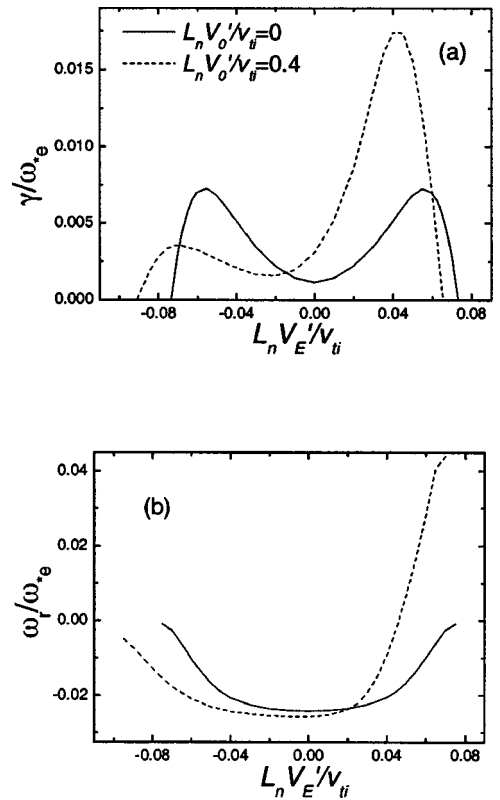


FIG. 9. The same as in Fig. 8 except for  $\beta_e = 0.05$ .

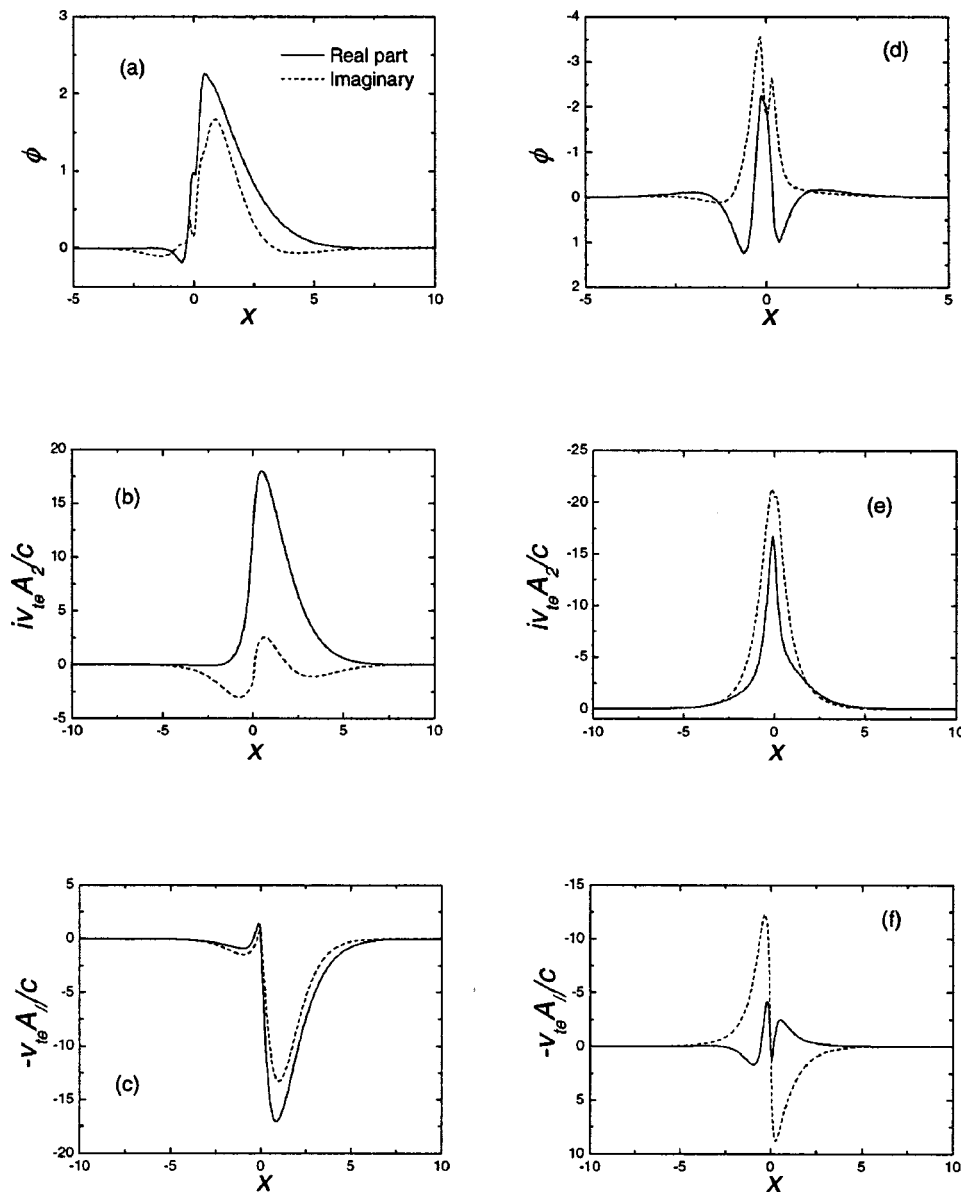


FIG. 10. The same as in Fig. 3 except that (a)–(c) are for  $\hat{V}'_E = 0.04$  and (d)–(f) are for  $\hat{V}'_E = -0.04$ .

by  $x/\rho_j$  in Eq. (9), higher efficiency of  $\hat{V}'_E$  is expected for the mode with more asymmetric structure. As noted in Secs. IV A and IV B, a positive  $\hat{V}'_0$  shifts the mode structure toward  $+x$  direction, as well as a positive  $\hat{V}'_E$  does. That is, at a given  $\hat{V}'_E$ , the mode structure with  $\hat{V}'_0 \hat{V}'_E > 0$  is more asymmetric than that without  $\hat{V}'_0$ , so the effect of sheared flow is strengthened. By contrast, the effect is weakened at  $\hat{V}'_0 \hat{V}'_E < 0$  since the asymmetries caused by flows with opposite signs counteract each other. Figure 10 shows the mode structures at  $\beta_e = 0.05$ ,  $\hat{V}'_0 = 0.4$ , and  $\hat{V}'_E = \pm 0.04$  while Fig. 3 shows the mode structures at  $\hat{V}'_0 = 0.4$  and  $\hat{V}'_E = 0$ . It is clear that the whole structure at  $\hat{V}'_E = +0.04$  is almost in the  $x > 0$  region while the structure at  $\hat{V}'_E = -0.04$  is nearly symmetric.

## V. SUMMARY AND DISCUSSION

We have derived a set of integral equations in Ref. 20 to study the slab drift instabilities in arbitrary  $\beta$  plasmas. In the

present paper, the equations are extended to investigate the effects of sheared flows on the ion temperature gradient mode. The sheared flow parameters include the ion parallel velocity shear, perpendicular velocity shear, current, and current gradient.

In summary, the parallel velocity shear is destabilizing while the destabilizing effect is weakened by finite  $\beta$ . The effects of current parameters are very weak not only for the electrostatics modes but also for the electromagnetic modes. The current in typical tokamak devices hardly influences the stability properties of the mode. The perpendicular velocity shear is stabilizing. Although the growth rate increases in low  $V'_E$  regime, a large enough  $\hat{V}'_E$  can completely stabilize the ion temperature gradient mode. Moreover, this effect is not weakened at finite even high  $\beta$ . At a weak magnetic shear, the destabilizing effect of the parallel velocity shear is further weakened while the stabilizing effect of the perpendicular velocity shear is highly strengthened. This trend is consistent with the experimental observations in

discharges<sup>1-3</sup> with internal transport barrier formation, where the transport barrier is built in the region with weak magnetic shear and strong sheared flows.

When the parallel and perpendicular sheared flows coexist, the flow effect can be stabilizing or destabilizing, depending on the relative sign of the velocity shears. However, the modes are completely stabilized for sufficiently large values of perpendicular velocity shear regardless of the signs. Sheared flows destroy the symmetry of mode structure. A positive  $\hat{V}'_E$  shifts the mode toward  $+x$  direction as does a positive  $V'_0$ . The mode has a relatively high growth rate but is stabilized by a relatively small  $V'_E$  for  $V'_0 V'_E > 0$ . This conclusion has been reached for electrostatic modes before<sup>12</sup> and is now verified and extended for arbitrary  $\beta$ .

From the results in the present work and Ref. 20, we can divide the plasma parameters into two groups. The first includes the magnetic shear and the perpendicular velocity shear, which can easily influence the stability property of the ITG mode at arbitrary  $\beta$ . The other includes the parallel velocity shear, parallel current, poloidal wavelength, and ion temperature gradient parameter, which hardly change the eigenfrequency and growth rate of the unstable mode at a high  $\beta$ . This also suggests that the magnetic shear and perpendicular velocity shear affects the modes mainly through the argument of the plasma dispersion function.

In this work, the parameters are chosen such that the parallel sheared flow is not so strong that the mode is dominantly driven by the ion temperature gradient. This is reasonable in ordinary conditions. For example, in DIII-D, parameters for the  $H$  mode are  $\eta_i \approx 2$  and  $\hat{V}'_0 \approx 0.12 \sim 0.25$ , while for the  $L$  mode  $\eta_i \approx 1$  and  $\hat{V}'_0 \approx 0.02 \sim 0.12$ .<sup>13</sup> If a stronger parallel sheared flow is adopted, many kinds of mode coupling may occur. It is found<sup>22</sup> that linear coupling occurs among the  $l=1, 2$ , and  $3$  modes, where  $l$  is the order of the radial eigenmode. If the parallel velocity shear is absent or weak, these modes have different mode structures and frequencies<sup>23</sup> and do not couple. This topic will not be further discussed here but may be an interesting topic in specific conditions.

## ACKNOWLEDGMENTS

The kind help of Professor H. Sanuki with the English in the paper is gratefully acknowledged.

This work was supported by the National Science Foundation of China, Grant Nos. 19889506 and 10135020.

- <sup>1</sup>E. J. Strait, L. L. Lao, M. E. Mauel, B. W. Rice, T. S. Taylor, K. H. Burrell, M. S. Chu, E. A. Lazarus, T. H. Osborne, S. J. Thompson, and A. D. Turnbull, Phys. Rev. Lett. **75**, 4421 (1995).
- <sup>2</sup>E. Mazzuato, S. H. Batha, M. Beer, R. E. Bell, R. V. Budny, C. Bush, T. S. Hahm, G. W. Hammett, F. M. Levinton, R. Nazikian, H. Park, G. Rewoldt, G. L. Schmidt, E. J. Synakowski, W. M. Tang, G. Taylor, and M. C. Zarnstorff, Phys. Rev. Lett. **77**, 3145 (1996).
- <sup>3</sup>Y. Koide, M. Kikuchi, M. Mori, S. Truji, S. Ishida, N. A. Sakura, Y. Kamada, T. Nishitani, Y. Kawano, T. Hatae, T. Fujita, T. Fukuda, A. Saka-sai, T. Kondoh, and Y. Neyatani, Phys. Rev. Lett. **72**, 3662 (1994).
- <sup>4</sup>K. H. Burrell, Phys. Plasmas **4**, 1499 (1997).
- <sup>5</sup>B. Coppi, M. N. Rosenbluth, and R. Z. Sagdeev, Phys. Fluids **10**, 582 (1967).
- <sup>6</sup>M. Greenwald, D. Gwinn, S. Milora, J. Parker, R. Parker, S. Wolfe, M. Besen, F. Camacho, S. Fairfax, C. Fiore, M. Foord, R. Gandy, C. Gomez, R. Granetz, B. La Bombard, B. Lipschultz, B. Lloyd, E. Marmor, S. McCool, D. Pappas, R. Petrasso, P. Pribyl, J. Rice, D. Schuresko, Y. Takase, J. Terry, and R. Watterson, Phys. Rev. Lett. **53**, 352 (1984).
- <sup>7</sup>S. D. Scott, P. H. Diamond, R. J. Fonck, R. B. Howell, K. P. Jahnig, G. Schilling, E. J. Synakowski, M. C. Zarnstorff, C. E. Bush, E. Fredrickson, K. W. Hill, A. C. Janos, D. K. Mansfield, D. K. Owens, H. Park, G. Pautasso, A. T. Ramsey, J. Schivell, G. D. Tait, W. M. Tang, and G. Taylor, Phys. Rev. Lett. **64**, 531 (1990).
- <sup>8</sup>P. J. Catto, M. N. Rosenbluth, and C. S. Liu, Phys. Fluids **16**, 1917 (1973).
- <sup>9</sup>J. Q. Dong, Y. Z. Zhang, S. M. Mahajan, and P. N. Guzdar, Phys. Plasmas **3**, 3065 (1996).
- <sup>10</sup>S. Hamaguchi and W. Horton, Phys. Fluids B **4**, 319 (1992).
- <sup>11</sup>G. Ganguli, Y. C. Lee, and P. J. Palmadesso, Phys. Fluids **31**, 823 (1988).
- <sup>12</sup>M. Artun and W. M. Tang, Phys. Fluids B **4**, 1102 (1992).
- <sup>13</sup>J. Q. Dong and W. Horton, Phys. Fluids B **5**, 1581 (1993).
- <sup>14</sup>X. Y. Fu, Ph.D. dissertation, Tsinghua University, 1997.
- <sup>15</sup>F. Wagner, Plasma Phys. Controlled Fusion **36**, A319 (1994).
- <sup>16</sup>A. Sykes, Nucl. Fusion **39**, 1271 (1999).
- <sup>17</sup>M. Ono, M. G. Bell, R. E. Bell *et al.*, Nucl. Fusion **41**, 1435 (2001).
- <sup>18</sup>M. Dobrowolny, Phys. Fluids **15**, 2263 (1972).
- <sup>19</sup>Z. Gao, J. Q. Dong, G. J. Liu, and C. T. Ying, Phys. Plasmas **8**, 4080 (2001).
- <sup>20</sup>Z. Gao, J. Q. Dong, G. J. Liu, and C. T. Ying, Phys. Plasmas **9**, 569 (2002).
- <sup>21</sup>S. Inoue, K. Itoh, and S. Yoshikawa, Nucl. Fusion **18**, 775 (1978).
- <sup>22</sup>Z. Gao, Ph.D. dissertation, Tsinghua University, 2002.
- <sup>23</sup>Z. Gao, J. Q. Dong, G. J. Liu, and C. T. Ying, Phys. Plasmas **9**, 1692 (2002).